

Article

Preparation of Biocomposite Soft Nanoparticles Composed of Poly(Propylene Oxide) and the Polymer-Binding Peptides

Toshiki Sawada ^{1,2}, Hiroki Fukuta ¹ and Takeshi Serizawa ^{1,*}

¹ Department of Chemical Science and Engineering, School of Materials and Chemical Technology, Tokyo Institute of Technology, 2-12-1-H121 Ookayama, Meguro-ku, Tokyo 152-8550, Japan; sawada@mac.titech.ac.jp (T.S.); hfukuta@polymer.titech.ac.jp (H.F.)

² Precursory Research for Embryonic Science and Technology, Japan Science and Technology Agency, 4-1-8 Honcho, Kawaguchi-shi, Saitama 332-0012, Japan

* Correspondence: serizawa@mac.titech.ac.jp

Received: 6 June 2020; Accepted: 13 July 2020; Published: 17 July 2020



Abstract: The molecular recognition capability of naturally occurring biomolecules is generally expressed against biomolecules in the biological milieu. Recently, it was demonstrated that the specific interactions of biomolecules such as short peptides were applicable to artificial materials. We have developed peptides with specific affinities for synthetic polymers toward functional biocomposite polymeric materials. In this study, we demonstrated the preparation of biocomposite nanoparticles composed of poly(propylene oxide) (PPO) and PPO-binding peptides. A simple injection of a concentrated PPO solution dissolved in an organic solvent into the peptide solution under sonication resulted in the formation of nanospherical structures. Morphological observation indicated characteristic softness and high applicability as a molecular carrier of the biocomposite nanoparticles. Structural characterization of PPO and the PPO-binding peptide revealed the structural conformability of these molecules to interact specifically with each other. Our findings expand the potential applicability of polymer-binding peptides for the future construction of biomedical materials composed of peptides and various polymers.

Keywords: polymer-binding peptide; phage display; polymeric nanoparticle; specific interaction; biomedical application

1. Introduction

Molecular recognition by biomolecules, especially peptides and proteins, is an essential molecular event to maintain biogeocenosis. The target molecules of such peptides and proteins are considered to be limited to natural biomolecules. Over the past two decades, various studies have revealed certain novel artificial peptides with specific affinities for artificial material compounds screened from a biologically constructed peptide library using phage or cell-surface display techniques [1–5]. These novel peptides specifically interact with the target materials through multiple noncovalent interactions such as hydrogen bonding, π -electron interactions, van der Waals interactions, and hydrophobic effects as natural peptides (or proteins) [6–15]. Therefore, it has been shown that these material-binding peptides recognize certain atomically or molecularly ordered three-dimensional arrangements of their target materials. We have developed peptides with a specific affinity for synthetic polymers for the construction of polymeric systems with the desired functionalization through polymer-binding peptides [16,17].

Traditionally, the functionalization of artificial materials, including polymers, through peptides has been performed on the liquid/solid surfaces of materials because the materials utilized are

solids. Our recent studies revealed that polymer-binding peptides enabled the functionalization of relatively hydrophilic synthetic polymers, of which states were dissolved in aqueous phase, well-dispersed in aqueous phases, or hydrogels [18–21]. For instance, the anticancer drug doxorubicin (Dox)-conjugated poly(propylene oxide) (PPO)-binding peptide (amino acid sequence: Asp-Phe-Asn-Pro-Tyr-Leu-Gly-Val-Thr-Pro-Val-Lys), of which the sequence was screened from a phage-displayed peptide library, was sustainably released from hydrogels composed of biomedically utilized block copolymers (poly(ethylene oxide) (PEO)-PPO-PEO (so-called Pluronic)) based on peptide affinity against target PPO segments [20]. As a result of the controlled release, sustained anticancer effects against human cancer cells were achieved. Furthermore, the Dox-conjugated peptide was loaded into the Pluronic micelles to effectively deliver Dox to human cancer cells [21]. These results strongly suggest the high potential applicability of polymer-binding peptides for various biomedical applications such as for controlled release and in drug delivery systems. To widen its applicability, construction of a peptide-based preparation system of biomedically utilizable polymeric materials is still required.

Recently, nanoparticles have gained considerable attention owing to their excellent thermal [22], electronic [23,24], and optical [25,26] properties. In fact, it has been reported that nanoparticles composed of various materials such as metals, metal oxides, ceramics, and polymers are relatively new particles, utilized in various material's fields [27–30]. In particular, polymeric nanoparticles generally show high biocompatibility and biodegradability, therefore, the preparation of polymeric nanoparticles and their functionalization are essential for nanoparticle-based biomedical applications. Although various methods for preparing polymeric nanoparticles, such as polymerization-induced nanoparticle formation and emulsification, have been established [31–34], simple but specific combination of polymeric components and biofunctional molecules for the preparation of nanoparticle is still challenging. We have developed a one-step preparation procedure of biocomposite polymeric nanoparticles composed of hydrophobic conjugated polymers and polymer-binding peptides [35,36]. Unique nanoparticles were prepared by the injection of concentrated polymer solutions with water-miscible organic solvents into aqueous peptide solutions under sonication conditions, resulting in the successful utilization of the peptide as a dispersant for the hydrophobic conjugated polymers and subsequent formation of composite nanoparticles. The applicability of this unique and simple method to prepare biocomposite nanoparticles for other polymers (such as the relatively hydrophilic PPO), however, is still unclear because of the weak hydrophobic interactions between PPO and the peptide.

Here, we demonstrate the polymer-binding peptide-based preparation of biocomposite PPO nanoparticles (Figure 1). A simple injection of a concentrated PPO/*N,N*-dimethyl formamide (DMF) solution into aqueous PPO-binding peptide solutions resulted in the formation of nanoparticles with a size of several tens of micrometers. Because larger aggregates were observed in the absence of the peptide or the presence of another peptide, the specific affinity of the PPO-binding peptide is essential for nanoparticle formation. Our results indicate that the strategy to utilize polymer-binding peptides as dispersants for nanoparticle formation showed a wide range of applications for various polymers to establish different bioprocesses.

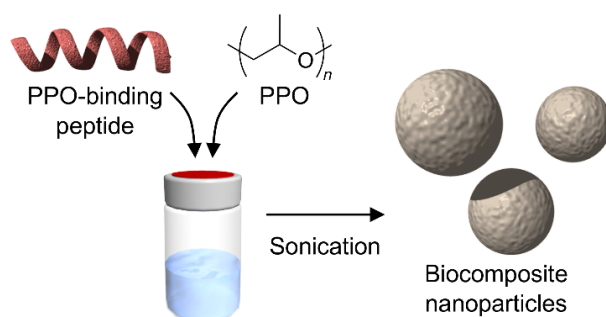


Figure 1. Schematic illustration of the preparation of biocomposite poly(propylene oxide) (PPO) nanoparticles with the PPO-binding peptide in an aqueous solution.

2. Materials and Methods

2.1. Materials

Dihydroxy-terminated PPO (M_n 7400, M_w/M_n 1.07) was purchased Polymer Source (Dorval, QC, Canada). All reagents for the peptide synthesis except for triisopropylsilane (TIS) were purchased from Novabiochem. TIS was purchased from Wako (Tokyo, Japan). EM stainer was purchased from Nisshin EM (Japan, Tokyo). NovaSynTGR resin and 9-fluorenylmethyloxycarbonyl (Fmoc) amino acid derivatives were purchased from Novabiochem (Burlington, MA, USA). All other reagents including organic solvents were purchased from Nacalai Tesque (Japan, Kyoto). Ultrapure water was produced at a resistivity greater than 18.2 M Ω by a Milli-Q Advantage A-10 apparatus (Millipore, Burlington, MA, USA).

2.2. Synthesis of Peptides

Peptides with a free *N*-terminus and an amidated *C*-terminus were prepared by solid-phase peptide synthesis using standard Fmoc-based procedures according to a previously published protocol [37]. Because the peptide was identified from a peptide library, which was displayed on the *N*-terminus of coat proteins of phage, the charge state was reflected by the *C*-terminal amidation of the peptide. The peptide chains were assembled on a NovaSynTGR resin (amino group 0.25 mmol g⁻¹) using Fmoc amino acid derivatives (3 equiv.) with 2-(1*H*-benzotriazole-1-yl)-1,1,3,3-tetramethyluronium hexafluorophosphate (3 equiv.), 1-hydroxybenzotriazole monohydrate (3 equiv.), and *N,N*-diisopropylethylamine (6 equiv.) in *N*-methylpyrrolidone (NMP) for coupling, and using 20% piperidine in NMP for the removal of Fmoc groups. To cleave the peptides from the resin and remove the protecting groups of side chains, the resins were treated with trifluoroacetic acid (TFA)/ultrapure water/TIS (9.5/0.25/0.25, v/v/v) for 2 h. The crude peptides were purified by reverse-phase high-performance liquid chromatography (ELITE LaChrom, HITACHI High-Technologies, Japan, Tokyo) using a C18 column (COSMOSIL 5C18-AR-300, 20 × 150 mm, Nacalai Tesque, Japan, Kyoto) with a linear gradient from 99.9% H₂O/0.1% TFA to 99.9% acetonitrile/0.1% TFA at a flow rate of 6 mL min⁻¹. The peptides were identified by liquid chromatography-mass spectrometry (LC-MS, Prominence UFLC system, MS-2020, Shimadzu, Japan, Kyoto).

2.3. Preparation of Nanoparticles

An aliquot (15 μ L) of DMF solution of PPO (0.333 mg/mL) was added to 985 μ L aqueous peptide solution (100 μ M in ultrapure water) under sonication (the final concentration of PPO was 0.5 μ g/mL). The mixed solution of peptides and PPO was sonicated for 1 h at 25 \pm 5 $^{\circ}$ C in a bath-type ultrasonic cleaner (55 W, USK-1R, AS ONE, Japan, Osaka). The mixtures were transferred to plastic microtubes and centrifuged at 10,000 \times *g* for 5 min at 25 $^{\circ}$ C to remove precipitated PPO. The supernatants were collected for further analysis.

2.4. Transmission Electron Microscopy (TEM) Observations

The surface of a collodion-coated copper EM grid (Nisshin EM) was modified to be hydrophilic via glow discharge treatments for 30 s (E-1010, Hitachi). An aliquot (10 μ L) of the supernatant was cast onto the modified grid. The samples were negatively stained by placing the sample side down onto the droplet of an EM stainer for 30 s. The grids were blotted and then allowed to dry at ambient temperature in a desiccator. All images were taken using a Hitachi H-7650 Zero. (HITACHI High-Technologies, Japan, Tokyo) An electron microscope operating at 100 kV.

2.5. Atomic Force Microscopy (AFM) Observations

An aliquot (10 μ L) of the supernatant was cast on a freshly cleaved mica substrate at ambient temperature. The samples were then applied to the observation. AFM images were obtained using an

SPM-9600 (Shimadzu) in tapping mode using standard silicon cantilevers. All images were scanned at a scan rate of 1 Hz with a maximum number of pixels (512×512). The AFM height analysis was performed at least three times to estimate an average value for each nanoparticle.

2.6. Dynamic Light Scattering (DLS) Measurements

An aliquot (70 μ L) of the nanoparticles in the supernatants was used for DLS measurements (Zetasizer Nano ZSP, Malvern) with a micro cell (DTS2145 Low volume glass cuvette, Malvern) at 25 °C. The measurement was performed after incubation for 5 min, 6 h, 12 h, or 24 h in the instruments at 25 °C.

2.7. Molecular Mechanics (MM) Calculations of the Structures of PPO and Peptides

MM calculations of PPO were performed using MM2 (PerkinElmer) and were started from the previously reported helical structures [38,39]. For the calculation size, PO (10 units) was used in this section. The calculated structure was compared to the structure of PPO-binding peptides [20] to estimate the structural suitability for the specific interaction.

3. Results and Discussion

The PPO-binding peptide was identified by LC-MS (Figure S1, M_w calcd 1347.7, m/z calcd $[M+H]^+$ 1348.7). The nanostructures of the dispersed objects were directly observed by TEM. Figure 2a shows a representative TEM image of the nanoobjects. The magnified TEM image demonstrated uniform spherical nanoparticles with a size of 65 ± 15 nm (the average diameter for 50 nanoparticles), demonstrating the single-step formation of biocomposite nanoparticles. When PPO was dispersed in an aqueous solution in the absence of the PPO-binding peptide, larger aggregates with irregular morphologies and sizes of sub-to-one micrometer were observed (Figure 2b). In the case of using the naphthalene-binding peptides (sequence: His-Phe-Thr-Phe-Pro-Gln-Gln-Gln-Pro-Pro-Arg-Pro), which have two aromatic amino acids (Phe residues) [40], large aggregates were also observed (Figure 2c). Because we have previously found that the aromatic amino acids (Phe2 and Tyr5) of the PPO-binding peptides were essential for the specific interactions with PPO [20], it strongly indicated that a simple bearing of aromatic amino acids to interact with other molecules through π -electron interactions and/or hydrophobic effects between peptides and PPO through aromatic amino acids is not essential for nanoparticle formation but, rather, specific interactions are necessary. Furthermore, when DMF was injected into the peptide solution (in the absence of PPO), aggregates with irregular morphologies and sizes of several hundreds of nanometers were observed (Figure 2d). The PPO-binding peptide dissolved well in an aqueous phase; therefore, such aggregates were considered to be prepared during the sample drying process. Larger aggregates of polymers and/or peptides were not observed in the TEM image of the supernatants of the PPO-binding peptide and PPO; these components were effectively used to form nanoparticles. These results show that biocomposite nanoparticles were successfully prepared through specific interactions between PPO and the PPO-binding peptides through suitable dispersion of PPO and subsequently for nanoparticles.

AFM observation was performed to characterize the nanoobjects in the supernatants. Representative AFM height images indicated the formation of nanoparticles composed of PPO and PPO-binding peptides (Figure 3a). The height of the nanoparticles was determined to be approximately 45 nm (Figure 3a, inset). The calculated height was slightly less than the diameter observed by TEM. This was probably because the nanoparticles were composed of relatively hydrophilic PPO and biomolecular peptides, which both have soft features, and were slightly squished by the tapping of the hard cantilevers during observation. Interestingly, the AFM phase images showed spherical structures with different color densities between the inner and outer areas as core-shell structures (Figure 3b). In this phase imaging, a paler color represents an area with more viscoelastic characteristics, and the peripheral part of the nanoparticle is considered to have a softer profile compared to the inside. We previously found that nanoparticles prepared using the same methodology using water-insoluble conjugated

polymers and their specific peptides have peptide-rich regions at the periphery of nanoparticles [35], possibly due to differences in solubility against an aqueous phase of the components. PPO also showed water-insoluble properties, whereas PPO has more hydrophilic chemical features than conjugated polymers; therefore, the nanoparticles in this study were also considered to have a composition distribution in spherical structures as in our previous study.

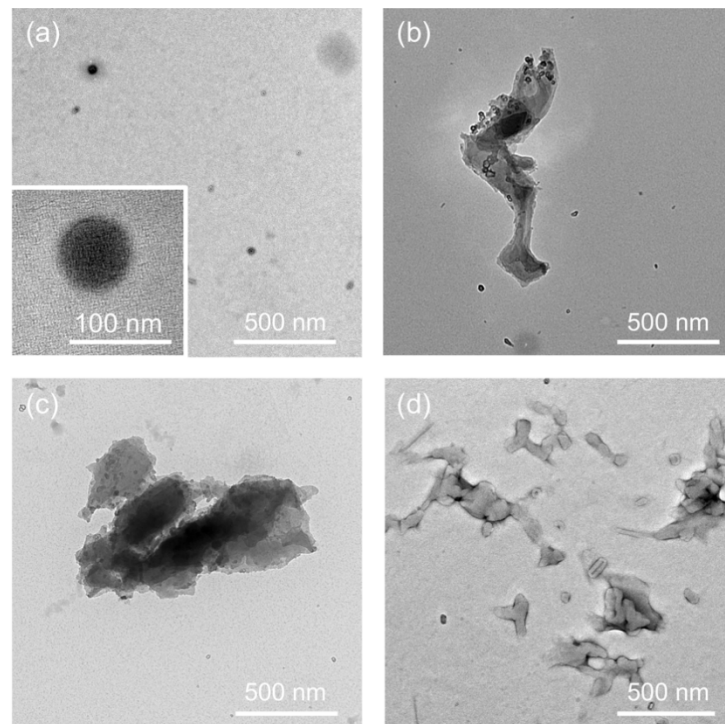


Figure 2. Transmission electron microscopy (TEM) images of the objects in the supernatants after sonication and subsequent centrifugation. (a) Biocomposite PPO nanoparticles prepared in the presence of PPO-binding peptide. (b) PPO aggregates prepared in the absence of peptides. (c) PPO aggregates prepared in the presence of the naphthalene-binding peptide. (d) Aggregates of the PPO-binding peptide.

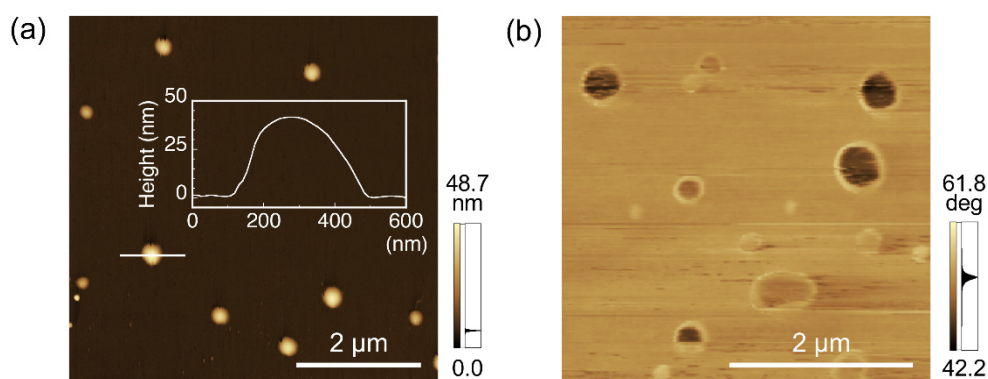


Figure 3. Atomic force microscopy (AFM) observation of the biocomposite nanoparticles using PPO and PPO-binding peptides. (a) Height image of biocomposite PPO nanoparticles prepared in the presence of the PPO-binding peptide. A representative cross-sectional analysis of the biocomposite nanoparticles is shown in the figure. (b) Phase image of biocomposite PPO nanoparticles observed in another position to (a).

DLS measurements were performed to characterize the hydrodynamic diameters of the biocomposite nanoparticles in an aqueous solution (Figure 4). The diameter of the nanoparticles was

approximately 170 nm after 5 min incubation, approximately three times greater than that observed by TEM and AFM. Because we observed dried nanoparticles by TEM and AFM, the possibility that the nanoparticles swelled in an aqueous phase could be derived from their hydrophilic features and/or existence of hydrated layers at the surface of the nanoparticles. The diameter of previously prepared nanoparticles composed of water-insoluble conjugated polymers and the peptides determined by DLS and TEM showed similar values (approximately 50 nm) [35], indicating softer characteristics and/or greater amounts of hydrated layers of the present nanoparticles. These results indicate that the nanoparticles prepared in this study have enough interior space to swell with water molecules as compared to those composed of more hydrophobic polymers, suggesting a high potential to efficiently carry drug molecules. The hydrodynamic diameters were almost the same during 24 h incubation, indicating high stability of the biocomposite nanoparticles. Furthermore, because the constituent polymeric structures used for nanoparticle formation drastically affected the resultant properties of the biocomposite nanoparticle, the precise design of polymers and specific peptides could expand the potential for many applications.

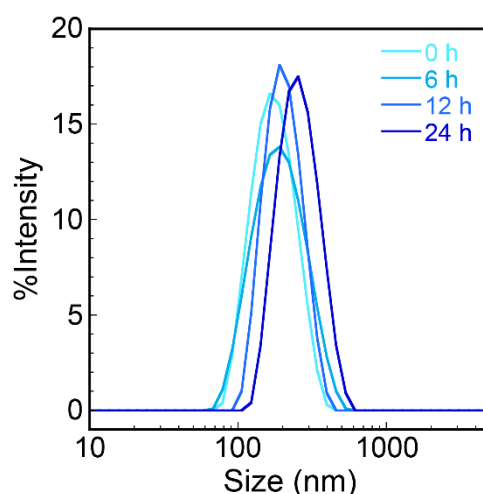


Figure 4. Time-dependent dynamic light scattering (DLS) measurements of the biocomposite nanoparticles composed of PPO and PPO-binding peptides.

In the previous sections, it was found that soft nanoparticles using PPO and PPO-binding peptides were successfully prepared. To obtain structural insights into the complex formation at the molecular level, MM calculations were performed for the PPO and PPO-binding peptides. We have previously reported that the PPO-binding peptide showed mixed secondary structures of random coil and α -helical structures by circular dichroism spectroscopy measurements and MM calculations, leading to the lateral aromatic groups of Phe2 and Tyr5 located on the same side [20]. The calculated PPO structure based on the previously reported helical structure [38,39] was compared with the structure of the PPO-binding peptide. The space-filling model of these possible structures suitably fitted to interact specifically with each other (Figure 5). We have also previously reported that CH- π interactions are essential for that specific interaction [20], and the possible structural fitting of these molecules through the side with aromatic amino acids of the peptide strongly suggested a suitable induced fit mechanism for specific interactions. This structural conformability of PPO and the PPO-binding peptide would be essential to form a stable biocomposite nanoparticle, and the strategy to utilize the desired polymers and their specific peptides for the establishment of bioapplicable processes shows the potential for biomedically utilized biocomposite materials in the near future.

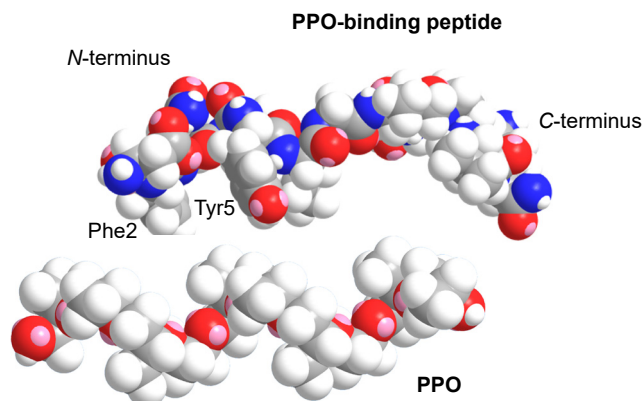


Figure 5. Structural comparison of PPO and PPO-binding peptides obtained from molecular mechanics (MM) calculations. Grey, white, blue, and red colors represent carbon, hydrogen, nitrogen, and oxygen molecules, respectively.

4. Conclusions

We demonstrated the preparation of biocomposite nanoparticles composed of PPO and PPO-binding peptides. Characterization of the nanoparticles indicated that the nanoparticles showed spherical structures with a size of approximately 170 nm in an aqueous phase, but only approximately 65 nm after the drying process. Such a difference was not observed in the combination of water-insoluble polymers and their specific peptides, demonstrating the soft characteristics and relatively greater carrying capability of the PPO-based biocomposite nanoparticle as compared to those prepared using hydrophobic polymers. The MM calculation strongly indicated that a structural fitting of these components for their specific interaction was essential for the resultant nanoparticle formation. Because the relatively hydrophilic PPO successfully formed nanospherical structures by the specific peptide-based dispersion, various synthetic polymers were considered to be appropriate for nanoparticle formation. Further utilization of suitably designed polymer-binding peptides would expand the potential applicability of peptide interaction-process-based nanoparticle formation. Our strategy to utilize polymer-binding peptides for the preparation of bioapplicable polymer-based materials will open new opportunities for the construction of designable composite biomaterials.

Supplementary Materials: The following are available online at <http://www.mdpi.com/2227-9717/8/7/859/s1>, Figure S1: Chromatogram and mass spectrum of the PPO-binding peptide after purification.

Author Contributions: T.S. (Takeshi Serizawa) directed and designed the project. T.S. (Toshiki Sawada) conceived and designed the experiments. T.S. (Toshiki Sawada) and H.F. analyzed the data. H.F. performed the experiments. T.S. (Toshiki Sawada) and T.S. (Takeshi Serizawa) cowrote the paper. All authors have read and agreed to the published version of the manuscript.

Funding: This work was supported in part by the Interdisciplinary Research Support for Scientists from Tokyo Tech for T. Sawada.

Acknowledgments: The authors wish to thank the technical support of TEM observations from the Open Facility Center, Materials Analysis Division (Tokyo Tech).

Conflicts of Interest: The authors declare no conflicts of interest.

References

1. Sarikaya, M.; Tamerler, C.; Jen, A.; Schulten, K.; Baneyx, F. Molecular biomimetics: Nanotechnology through biology. *Nat. Mater.* **2003**, *2*, 577–585. [[CrossRef](#)] [[PubMed](#)]
2. Joseph, M.S.; Rajesh, R.N. Probing peptide-nanomaterial interactions. *Chem. Soc. Rev.* **2010**, *39*, 3454–3463.
3. Baneyx, F.; Schwartz, D. Selection and analysis of solid-binding peptides. *Curr. Opin. Biotechnol.* **2007**, *18*, 312–319. [[CrossRef](#)]
4. Walsh, T.R.; Knecht, M.R. Biointerface Structural Effects on the Properties and Applications of Bioinspired Peptide-Based Nanomaterials. *Chem. Rev.* **2017**, *117*, 12641–12704. [[CrossRef](#)] [[PubMed](#)]

5. Limo, M.J.; Sola-Rabada, A.; Boix, E.; Thota, V.; Westcott, Z.C.; Puddu, V.; Perry, C.C. Interactions between Metal Oxides and Biomolecules: From Fundamental Understanding to Applications. *Chem. Rev.* **2018**, *118*, 11118–11193. [[CrossRef](#)]
6. Sarikaya, M.; Tamerler, C.; Schwartz, T.D.; Baneyx, F. Materials assembly and formation using engineered polypeptides. *Annu. Rev. Mater. Res.* **2004**, *34*, 373–408. [[CrossRef](#)]
7. Guinay, K.; Klok, H.-A. Identification of Soft Matter Binding Peptide Ligands Using Phage Display. *Bioconjugate Chem.* **2015**, *26*, 2002–2015. [[CrossRef](#)]
8. Sawada, T.; Mihara, H. Dense surface functionalization using peptides that recognize differences in organized structures of self-assembling nanomaterials. *Mol. BioSyst.* **2012**, *8*, 1264–1274. [[CrossRef](#)]
9. Sawada, T.; Serizawa, T. Immobilization of Highly-Oriented Filamentous Viruses onto Polymer Substrates. *J. Mater. Chem. B* **2013**, *1*, 149–152. [[CrossRef](#)]
10. Sano, K.-I.; Shiba, K. A hexapeptide motif that electrostatically binds to the surface of titanium. *J. Am. Chem. Soc.* **2003**, *125*, 14234–14239. [[CrossRef](#)]
11. Hayashi, T.; Sano, K.-I.; Shiba, K.; Kumashiro, Y.; Iwahori, K.; Yamashita, I.; Hara, M. Mechanism underlying specificity of proteins targeting inorganic materials. *Nano Lett.* **2006**, *6*, 515–524. [[CrossRef](#)]
12. Tamerler, C.; Oren, E.; Duman, M.; Venkatasubramanian, E.; Sarikaya, M. Adsorption kinetics of an engineered gold binding Peptide by surface plasmon resonance spectroscopy and a quartz crystal microbalance. *Langmuir* **2006**, *22*, 7712–7720. [[CrossRef](#)]
13. Seker, U.; Wilson, B.; Dincer, S.; Kim, I.; Oren, E.; Evans, J.; Tamerler, C.; Sarikaya, M. Adsorption behavior of linear and cyclic genetically engineered platinum binding peptides. *Langmuir* **2007**, *23*, 7895–7900. [[CrossRef](#)] [[PubMed](#)]
14. Wang, S.; Humphreys, E.S.; Chung, S.-Y.; Delduco, D.F.; Lustig, S.R.; Wang, H.; Parker, K.N.; Rizzo, N.W.; Subramoney, S.; Chiang, Y.-M.; et al. Peptides with selective affinity for carbon nanotubes. *Nat. Mater.* **2003**, *2*, 196–200. [[CrossRef](#)]
15. Kase, D.; Kulp, J.; Yudasaka, M.; Evans, J.; Iijima, S.; Shiba, K. Affinity selection of peptide phage libraries against single-wall carbon nanohorns identifies a peptide aptamer with conformational variability. *Langmuir* **2004**, *20*, 8939–8941. [[CrossRef](#)] [[PubMed](#)]
16. Serizawa, T.; Matsuno, H.; Sawada, T. Specific interfaces between synthetic polymers and biologically identified peptides. *J. Mater. Chem.* **2011**, *21*, 10252–10260. [[CrossRef](#)]
17. Sawada, T.; Mihara, H.; Serizawa, T. Peptides as new smart bionanomaterials: Molecular recognition and self-assembly capabilities. *Chem. Rec.* **2013**, *13*, 172–186. [[CrossRef](#)]
18. Suzuki, S.; Sawada, T.; Ishizone, T.; Serizawa, T. Affinity-based thermoresponsive precipitation of proteins modified with polymer-binding peptides. *Chem. Commun.* **2016**, *52*, 5670–5673. [[CrossRef](#)]
19. Suzuki, S.; Sawada, T.; Ishizone, T.; Serizawa, T. Bioinspired structural transition of synthetic polymers through biomolecular ligand binding. *Chem. Commun.* **2018**, *54*, 12006–12009. [[CrossRef](#)]
20. Serizawa, T.; Fukuta, H.; Date, T.; Sawada, T. Affinity-based release of polymer-binding peptides from hydrogels with the target segments of peptides. *Chem. Commun.* **2016**, *52*, 2241–2244. [[CrossRef](#)]
21. Sawada, T.; Takizawa, M.; Serizawa, T. Affinity-based Functionalization of Biomedically Utilized Micelles Composed of Triblock Copolymers through Polymer-binding Peptides. *ACS Biomater. Sci. Eng.* **2019**, *5*, 5714–5720. [[CrossRef](#)]
22. Andrievskii, R. Review of thermal stability of nanomaterials. *J. Mater. Sci.* **2014**, *49*, 1449–1460. [[CrossRef](#)]
23. Yonezawa, T.; Uchida, K.; Yamanoi, Y.; Horinouchi, S.; Terasaki, N.; Nishihara, H. Room-temperature immobilization of gold nanoparticles on Si(111) surface and their electron behaviour. *Phys. Chem. Chem. Phys.* **2008**, *10*, 6925–6927. [[CrossRef](#)]
24. Minea, A.A. A Review on Electrical Conductivity of Nanoparticle-Enhanced Fluids. *Nanomaterials* **2019**, *9*, 1592. [[CrossRef](#)]
25. Herbani, Y.; Nakamura, T.; Sato, S. Synthesis of Near-Monodispersed Au–Ag Nanoalloys by High Intensity Laser Irradiation of Metal Ions in Hexane. *J. Phys. Chem. C* **2011**, *115*, 21592–21598. [[CrossRef](#)]
26. Kelly, K.L.; Coronado, E.; Zhao, L.L.; Schatz, G.C. The Optical Properties of Metal Nanoparticles: The Influence of Size, Shape, and Dielectric Environment. *J. Phys. Chem. B* **2003**, *107*, 668–677. [[CrossRef](#)]
27. Wilson, R. The use of gold nanoparticles in diagnostics and detection. *Chem. Soc. Rev.* **2008**, *37*, 2028–2045. [[CrossRef](#)] [[PubMed](#)]

28. Sardar, R.; Funston, A.; Mulvaney, P.; Murray, R. Gold nanoparticles: Past, present, and future. *Langmuir* **2009**, *25*, 13840–13851. [[CrossRef](#)] [[PubMed](#)]
29. Alkilany, A.; Lohse, S.; Murphy, C. The Gold Standard: Gold Nanoparticle Libraries To Understand the Nano-Bio Interface. *Acc. Chem. Res.* **2012**, *46*, 650–661. [[CrossRef](#)] [[PubMed](#)]
30. Khan, I.; Saeed, K.; Khan, I. Nanoparticles: Properties, applications and toxicities. *Arab. J. Chem.* **2019**, *12*, 908–931. [[CrossRef](#)]
31. Akutsu, Y.; Taguchi, Y.; Tanaka, M. Preparation of Composite Particles by Forming Pickering Emulsion Followed by Drying-In-Liquid and Effect of Stepwise Addition of Solid Powder on Structure of Composite Particles. *Mater. Sci. Appl.* **2013**, *4*, 786–793. [[CrossRef](#)]
32. Jelvehgari, M.; Siah-Shadbad, M.R.; Azarmi, S.; Gary, P.M.; Ali, N. The microsp sponge delivery system of benzoyl peroxide: Preparation, characterization and release studies. *Int. J. Pharm.* **2006**, *308*, 124–132. [[CrossRef](#)] [[PubMed](#)]
33. Andrew, G.M.; Klaus, M. Molecularly Imprinted Polymer Beads: Suspension Polymerization Using a Liquid Perfluorocarbon as the Dispersing Phase. *Anal. Chem.* **1996**, *68*, 3769–3774.
34. Lichti, G.; Hawkett, B.S.; Gilbert, R.G.; Napper, D.H.; Sangster, D.F. Styrene emulsion polymerization: Particle-size distributions. *J. Polym. Sci. Polym. Chem.* **1981**, *19*, 925–938. [[CrossRef](#)]
35. Ejima, H.; Matsumiya, K.; Sawada, T.; Serizawa, T. Conjugated polymer nanoparticles hybridized with the peptide aptamer. *Chem. Commun.* **2011**, *47*, 7707–7709. [[CrossRef](#)] [[PubMed](#)]
36. Sawada, T.; Matsumiya, K.; Serizawa, T. Polymer-binding Peptides as Dispersants for the Preparation of Polymer Nanoparticles: Application of Peptides to Structurally Similar Non-target Polymers. *Chem. Lett.* **2015**, *44*, 831–833. [[CrossRef](#)]
37. Chan, W.C.; White, P.D. *Fmoc Solid Phase Peptide Synthesis*, 1st ed.; Chan, W.C., White, P.D., Eds.; Oxford University: New York, NY, USA, 2000; pp. 41–76.
38. Eunji, L.; Ja-Hyoung, R.; Myoung-Hwan, P.; Myongsoo, L.; Kyung-Hee, H.; Yeon-Wook, C.; Byoung-Ki, C. Observation of an unprecedented body centered cubic micellar mesophase from rod-coil molecules. *Chem. Commun.* **2007**, 2920–2922. [[CrossRef](#)]
39. Hong, D.J.; Lee, E.; Jeong, H.; Lee, J.K.; Zin, W.C.; Nguyen, T.D.; Glotzer, S.C.; Lee, M. Solid-State Scrolls from Hierarchical Self-Assembly of T-Shaped Rod-Coil Molecules. *Angew. Chem. Int. Ed.* **2009**, *48*, 1664–1668. [[CrossRef](#)]
40. Sawada, T.; Okeya, Y.; Hashizume, M.; Serizawa, T. Screening of peptides recognizing simple polycyclic aromatic hydrocarbons. *Chem. Commun.* **2013**, *49*, 5088–5090. [[CrossRef](#)]



© 2020 by the authors. Licensee MDPI, Basel, Switzerland. This article is an open access article distributed under the terms and conditions of the Creative Commons Attribution (CC BY) license (<http://creativecommons.org/licenses/by/4.0/>).